Tanzania Journal of Engineering and Technology 2023, **42**(**1**):85-96
OPEN ACCESS articles distributed under Creative Commons Attribution Licence [CC BY-ND]
Websites: https://ajol.org/tjet; https://tjet.udsm.ac.tz

ISSN 1821-536X (**print**); ISSN 2619-8789 (**electronic**)
https://doi.org/10.52339/tjet.v42i1.891

Special Issue – Seventh International Conference on Mechanical and Industrial Engineering (MIE) 2022 Conference, 20 – 21, October 2022, University of Dar es Salaam New Library, Dar es Salaam, TANZANIA

Studying Dielectric Losses of Serially Combined Silicone Rubber and Epoxy Resin

Aviti Thadei Mushi[†], **Jackson J. Justo and Alexander Kyaruzi**

Department of Electrical Engineering, University of Dar es Salaam, Dar es Salaam, Tanzania

[†]Corresponding author: aviti.thadei@udsm.ac.tz, aviti.bahati@gmail.com;

ORCID: https://orcid.org/0000-0002-2958-2919

ABSTRACT

High voltage outdoor insulation systems are conventionally ceramics and glass with several advantages, such as proven in the field, excellent dielectric properties, durability, and long life. However, they are heavy, attract vandals and break easily, and they can lose their dielectric properties easily when subjected to high voltage transients, arcing, and surges. To curb this, polymer insulators are used because they have excellent dielectric properties, such as those of ceramics and glass, with the added advantages that they do not break easily and recover their lost dielectric properties after any electrical transients. Therefore, this paper investigates the dielectric properties of polymeric materials – silicone rubber (SR) and epoxy resin (ER). Some SR samples were manufactured in the laboratory, and others were obtained from the industrial manufacturer. All the ER samples were manufactured in the laboratory. The dielectric measurements were performed with the Insulation Diagnostics System. Within the measured frequency ranges, the dielectric losses of SR manufactured industrially differ from the laboratory-manufactured specimens. This is due to filler materials in the industrially manufactured samples. For the case of serially connecting the SR and ER, there was a higher influence of dielectric loss of SR than the ER, with some remarkable dielectric losses at some frequencies.

ARTICLE INFO

First submitted: June 29, 2022

Revised: Sep. 29, 2022

Presented: Oct. 21 - 22, 2022

Accepted: Dec. 15, 2022

Published: February 25, 2023

Keywords: *polymers, insulation, relaxation, losses, high voltage*

INTRODUCTION

Polymeric materials are increasingly becoming popular worldwide in applications of outdoor high-voltage insulators; therefore, it is imperative to study their dielectric properties (Boudefel & Gonon, 2006; Ehsani et al., 2007; Wang et al., 2000). These days, excellent polymer insulators have worked effectively in transmission lines. There are various reports on the dielectric properties of polymer insulators' investigation (Ediriweera et al., 2020; Mushi & Kyaruzi, 2022; Tuncer, 2005). These measurements give information about the molecular, ionic, and electronic state of the dielectric material, all of which are crucial for the effective application of polymer insulators to outdoor environments (de Andrade Raponi et al., 2018; Jonscher, 1999; Nguyen et al., 2004; Zong et al., 2005).

These researches are vital since they inform about diagnostic tools of outdoor polymeric insulators (Nixdorf & Busse, 2001; Thadei, 2010), their conductivity (Thadei & Kyaruzi, 2008; Tuncer & Gubanski, 1999, 2000), any damage to the molecular structures (Serdyuk et al., 2002; Tuncer, 2004, 2005), useful to detect ageing effects (Kumara et al., 2022; Seifert et al., 1998), and any presence of mechanical failures of the central rod (Ogbonna et al., 2022). Epoxy resin (ER) forms the polymer matrix (Uflyand et al., 2022). Polymer insulators are widely the choice of high voltage engineers because they can be made UV radiation resistant (Francis & Philip, 2022). In this article, dielectric loss tangent (tan δ) of single and series SR and ER specimens have been investigated. Seifert et al. (1998) reported dielectric measurements which showed material damages due to electrical over-stresses such as those discussed by Choudhary et al. (2022) and Ediriweera et al. (2020), respectively, and developed an effective tool to detect and classify the ageing in composite polymeric insulations. These were the results of the interactions at the large internal filler surfaces showing an increment in the conductivity and intensification of interfacial polarizations. These effects, when acting in tandem with the electrical service stress, can lead to the detachment of the internal filler resin bonding, which increases the tan δ and a simultaneous decrease of the electrical strength and life-span (Rodríguez-Serna & Albarracín-Sánchez, 2021). The work by Das-Gupta and Scarpa, quoted by Seifert et al. (1998), used an extremely low-frequency dielectric diagnostic tool to investigate the insulation of AC-aged XLPE high-voltage cables. This paper's dielectric measurements were undertaken in the low-frequency ranges and were impactful in assessing the cable insulation.

These dielectric spectroscopy measurements of insulation materials provide the status of internal condition. This technique is used in various branches of science to provide information on the structural and dynamical properties of considered material systems. This technique enables the studies of polarization mechanisms in the time and frequency domain (Riande & Díaz-Calleja, 2004; Seifert et al., 1998; Thadei, 2010). For high-voltage insulators, moisture ingress information is obtained. It has been established in many research findings that moisture ingress destroys insulation properties and shortens the lifetime of insulation material. In this study by Thadei & Kyaruzi (2008), the charge trapping by filler particles was observed at lower frequencies. These spectroscopy measurements show the molecular structure portrayed as the orientation of dipoles under the action of an electric field; the experimental devices used for this task can cover the frequency range of 10^{-4} to 10^{11} Hz (Jonscher, 1999). But note that one instrument cannot cover this frequency range, so it has to be a combination of instruments to obtain meaningful results.

In the current work, the range covered by the instrument used was 10^{-4} to 10^{3} Hz, so no other instrument is needed for the measurements. Through these, the dielectric characteristics of polymeric insulation materials are investigated.

LITERATURE REVIEW

Dielectric Properties of Polymer Materials

Some researchers, including Asokan et al., (2020), Kumara et al. (2022), and Serdyuk et al. (2002), compared computer simulations and experimental dielectric measurements and observed pronounced complex permittivity of one of the insulation materials. They observed other interesting phenomena regarding the relaxation of these materials in the frequencies of 10 mHz – 1 Hz. These showed that the computer simulation is good for qualitatively estimating the

dielectric properties. Others, such as Tuncer & Gubanski (1999, 2000) and Wu et al. (2019), investigated mixtures (composites) of SR with Aluminium Trihydrate (ATH) filler. These results show that the SR's conductivity at various temperatures is impacted. These high concentrations of ATH fillers act as charge traps within the materials at higher temperatures. Further, Nguyen et al. (2004) identified two polarization mechanisms within SRs filled with silica; one was a hopping charge transport at moderate to higher electric fields. Dakin (2006 discussed mechanisms of the magnitude and the issues of polarization and conduction in dielectric materials. These discussions focused on molecular and physical structure, frequency, and operating temperature in the outdoor environment. Charge transport studies are crucial when designing high-performance polymers (Jia et al., 2022).

The AC and DC conductivity of polymers are impacted by increasing temperature, while the AC conductivity varies with frequency (Bright, 2013; Li, Shahsavarian, et al., 2021). Conduction, dielectric constant, and polarization are related to a material's electrical properties(Jonscher, 1999). There are four principal types of polarizations within an insulation material: electronic, ionic-interfacial, atomic-ionic displacement, and dipolar.

Dielectric Polarization

The electronic polarization phenomena within an insulator occur over a wide frequency, from DC frequency up to optical frequencies. The second polarization, which is ionic-interfacial, manifests itself in lower frequencies slightly above the DC frequency. The third polarization mechanism, which is atomic-ionic, follows the electronic polarization, occurring from DC up through optical frequencies. The fourth polarization occurs from DC up through infrared (IR) frequencies. It is dominant in materials such as inorganic crystals, glasses, and ceramics. The fifth polarization, called dipolar polarization covers the frequency range from DC up to microwave frequencies. Due to the application of an electric field manifests depending on the presence of dipolar molecules and the inertial to rotate these molecules. Important polarizations are the ionic-interfacial and dipolar occurring for most organic liquids and resins used as electrical insulators at commonly working frequencies. These two polarization mechanisms are associated with conduction and dielectric losses. The molecular dipole polarization contributes to dielectric constant and short-time conduction in insulators at lower AC frequencies. Major and/or minor impurities within an insulator cause dipolar molecules polarization in insulating liquids or resins (Dakin, 2006; Nguyen et al., 2004; Riande & Díaz-Calleja, 2004). An electric field causes a torque on a polymer material that tends to align these dipoles to its direction, causing rotation of the dipoles (Riande & Díaz-Calleja, 2004; Seanor, 1982). The rotation causes a short-time current to pass through the polymers.

METHODS AND MATERIALS

The methods, materials, and tools used to carry out this study are covered in this Section.

Tools for Measuring Dielectric Properties

The frequency dielectric spectroscopy experiments on the polymer insulation materials utilized the Insulation Diagnostics Systems (IDA 200 Programma) (GE Energy Services, 2007) with the Keithley Resistance Test Fixture (Keithley Model 8009) (Instruments LLC, 2019).

Dielectric Properties of a Polymer under the Action of an Electric Field

Applying an electric field to an insulator enables synthesizing the relationship between dielectric loss ($\tan\delta$) and complex permittivity (ε^*) of that material. The ε^* is given by:

$$\varepsilon^*(w) = \varepsilon'(w) - j\varepsilon''(w), \quad (1)$$

for single relaxation time materials, as a function of complex frequency w, as will be shown later, their ε^* will be given by Equation (2), whereby the real part ε' is given in Equation (3), and the imaginary part ε'' is given in Equation (4).

$$\varepsilon^*(w) = \varepsilon_\infty + \frac{\varepsilon_o - \varepsilon_\infty}{1 + jw\tau} \quad (2)$$

$$\varepsilon'(w) = \varepsilon_\infty + \frac{(\varepsilon_o - \varepsilon_\infty)}{1 + w^2\tau^2} \quad (3)$$

$$\varepsilon''(w) = \frac{(\varepsilon_o - \varepsilon_\infty)w\tau}{1 + w^2\tau^2} \quad (4)$$

Then, the $\tan\delta$ is defined by Equation (5) – (6), where the ε_o is the permittivity at higher frequencies, ε_∞ is the permittivity at lower frequencies. The Debye macroscopic relaxation time is represented by τ within (2) – (4). These equations have been dubbed the Debye equations for permittivity, relating it to the dielectric loss of an insulating material.

$$\tan\delta(w) = \frac{\varepsilon''(w)}{\varepsilon'(w)} \quad (5)$$

$$\tan\delta(w) = \frac{(\varepsilon_o - \varepsilon_\infty)\, w\tau}{\varepsilon_o + \varepsilon_\infty w^2\tau^2} \quad (6)$$

However, Equation (2) applies to polymers made by very short chains and enough dipoles, as pointed out by these (Jonscher, 1999; Nguyen et al., 2004). They argue that for practical polymer insulators, the Debye relaxation time is a distributed parameter; therefore, the complex permittivity will become Equation (7). The shape parameter is represented by the symbol β which distributed those relaxation times.

$$\varepsilon^*(w) = \varepsilon_\infty + \frac{\varepsilon_o - \varepsilon_\infty}{1 + (jw\tau)^{1-\beta}}, \quad (7)$$

where $0 < \beta < 1$. Equation (7) shows different relaxation times within an insulating polymer. These relaxation times are observed all lying close to each other, which can be termed polarized chains of polymers with different chain lengths or dipoles moments upon scrutiny. This behaviour is called non-Debye relaxation. Therefore, when one engages in measuring dielectric properties, they are forced to utilise time domain and frequency domain measuring devices. However, superior measuring devices work in the frequency domain (Instruments LLC, 2019). A polymer insulating material (condenser) in a disc shape is placed between the circular electrodes of a measuring device (Figure 1). The current that traverses the condenser is given by Equation (8), where I^* (or I) is the total current and G is the conductance of that insulating polymer material. The applied step voltage presents the capacitance; equivalently, that total current through the condenser can be written as Equation (9a) or expanded as Equation (9b).

$$I^* = (G + jwC)V_o \quad (8)$$

$$\frac{I^*(w)}{V_o} = jwC_o\varepsilon^* = Y^* \quad (9a)$$

$$I^*(w) = jV_oC_o(\varepsilon'(w) + \varepsilon''(w)) \quad (9b)$$

Equations (9a) and (9b) contain the complex admittance, Y^*, of the dielectric material under test, with the vacuum capacitance C_o expressed by Equation (10). The vacuum permittivity is ε_0, the tested dielectric material disc surface area covered by the electrodes is A, and d is its thickness, see Figure 1.

$$C_o = \frac{\varepsilon_o A}{d} \quad (10)$$

The voltage source impresses V_1 the condenser sample, out of which the power converter ($I-V$) changes the current I into voltage V_2. The instrument compares the amplitude and the phase angle between

two voltages (V_1 and V_2), then computes the complex impedance Z_s of the material under test, shown by Equation (11); the resistor R is the one used for voltage-to-current conversion, is within the instrument.

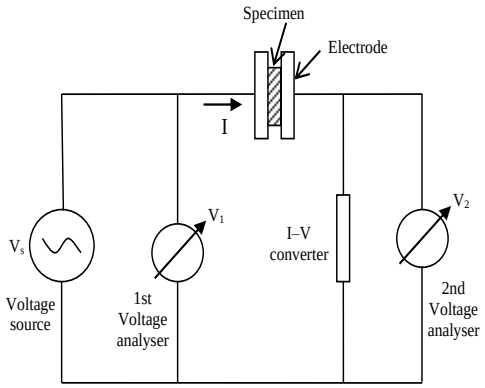

Figure 1: Dielectric frequency analyser equivalent circuit diagram
Source: (Instruments LLC, 2019)

$$Z_s = \frac{V_1 - V_2}{I_s} = \frac{V_1 - V_2}{V_2} R \tag{11}$$

Series and Parallel Dielectric Networks of an Insulating Material

To simplify the analysis, the insulation material discs can be modelled as a simple circuit of RC networks: parallel and series (Figure 2). The insulation material model has equivalent resistance and capacitance $C_i,\ i = \{s, p\}$ shown in Figure 2; the subscript *s* and *p* signify series or parallel, respectively.

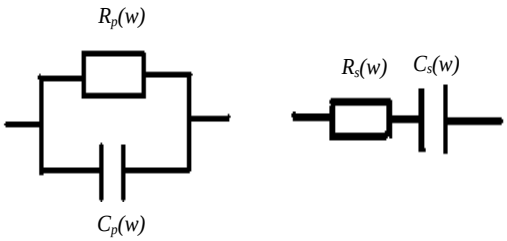

Figure 2: Simple RC networks – (a) parallel and (b) series models.

Equivalence between the series and parallel RC networks is achieved by making admittance Y^* (Equation (12)) equal to the impedance Z_s reciprocal (Equation (13).

$$Y^* = R^{-1}{}_p + jwC_p \tag{12}$$

$$Z_s = R_s + \frac{1}{jwC_s} \tag{13}$$

The equivalence condition between the series and parallel models is depicted by (14a) – (14e), from which the dielectric loss is obtained by Equation (14f) for some specific frequency ranges. The conductance of the polymer network is represented by G.

$$R^{-1}{}_p = G = \frac{R_s}{R^2{}_s + (wC_s)^{-2}} \tag{14a}$$

$$R_p = R_s\left(1 + \frac{1}{(wC_sR_s)^{-2}}\right) \tag{14b}$$

$$C_p = \frac{C_s}{1 + (wC_sR_s)^2} \tag{14c}$$

$$R_s = \frac{R_p}{1 + (wC_pR_p)^{-2}} = \frac{G}{G^2 + (wC_p)^2} \tag{14d}$$

$$C_s = C_p\left(1 + \frac{G^2}{(wC_p)^2}\right) \tag{14e}$$

$$\tan\delta(w) = wC_sR_s = \frac{1}{wR_pC_p} \tag{14f}$$

The arrangement of Figure 1 shows an electric field applied to an insulating material (polymers for this study) which exhibits one relaxation time shown in Figure 3, a Maxwell-Wagner polarization (Kumara et al., 2020; Li, Chen, et al., 2021; Xu et al., 2017). The shown parallel capacitance $C_{t\approx 0}$ is the high-frequency polarization capacitance, which is strange, independent of the frequency bands. This leads to modelling the series of RC circuits as a single relaxation time material with this constant dubbed the Maxwell-Wagner Time constant τ_{MW} given by Equation (15). This is adequate to model a polymeric material such as SR or ER or their arrangements, as this study did.

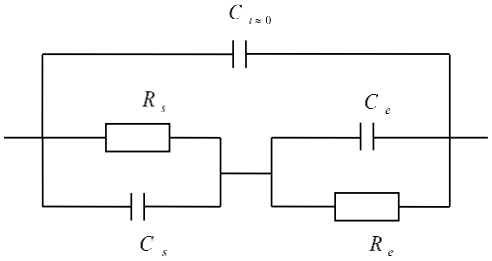

Figure 3: Circuit analogue of electrical insulation system modelled as a single relaxation time insulator (Blythe & Bloor, 2005; Capaccioli et al., 1998; Dakin, 2006).

$$\tau_{mw} = \frac{R_s R_e (C_s + C_e)}{R_s + R_e} \quad (15)$$

The Conductance of Polymer Insulators

In the analogue circuits for the polymers, the resistances represent conductivity; thus σ^* and ε^* are related by Equation (16).

$$\sigma^*(w) = \sigma' + j\sigma'' = \varepsilon_o w\varepsilon'' + jw\varepsilon' \quad (16)$$

The conductivity's real part $\sigma' = \varepsilon_0 w\varepsilon''$ represents the $\tan\delta$, and conductivity's imaginary part $\sigma'' = \varepsilon_0 w\varepsilon'$ represents the displacement current, manifesting as dielectric losses. Log-log plots of $\tan\delta$ Vs w shows an inverse relationship in low-frequency regions due to DC conductivity (Riande & Díaz-Calleja, 2004; Seanor, 1982).

Specimen Manufacturing

There were silicone rubber (S, SF, and PS) specimens and epoxy resin (E) specimens. Specimens were manufactured at the Materials Laboratory in at Chalmers University of Technology, and some were delivered by manufacturers delivered some. The conditions of manufacturing and the dimensions of specimens are given in Table 1. The meaning of the abbreviations of sample names in Table 1 is explained in length elsewhere (Thadei, 2010; Thadei & Kyaruzi, 2008).

Table 1: Polymer samples manufacturing parameters

Specimen	Material	Name	1st curing time and temperature	2nd curing time and temperature	Thickness
Epoxy resin specimens	Araldite	E141	4 hours at 80°C	10 hours at 130 °C	1.2 mm
	Araldite	E142	4 hours at 80°C	10 hours at 130 °C	1.2 mm
	Araldite	E241	4 hours at 80°C	20 hours at 130 °C	1.2 mm
	Araldite	E242	4 hours at 80°C	20 hours at 130 °C	1.2 mm
	Araldite	E481	4 hours at 80°C	44 hours at 130 °C	1.6 mm
	Araldite	E482	4 hours at 80°C	44 hours at 130 °C	1.4 mm
Silicone rubber specimens	Sylgard 184	S1	120 minutes at 120 °C		1.0 mm
	Sylgard 184	S2	120 minutes at 120 °C		1.0 mm
	Sylgard 184	S481	48 hours at 22-25 °C		1.0 mm
	Sylgard 184	S482	48 hours at 22-25 °C		1.0 mm
	Dow corning pressed	SF1	High Temperature Vulcanised (HTV) rubber		3.0 mm
	Dow corning pressed	SF2	HTV rubber		3.0 mm
	PowerSil	PS	HTV rubber		2.0 mm

Spectroscopy Measurements

The frequency spectroscopy measurements were done using the Insulation Diagnostics System (IDA 200 Programma), which used the Resistivity Test Fixture (Keithley model 8009). This fixture has ring electrodes. The testing conditions were room temperature (22 ˚C – 25 ˚C) and humidity of 32% – 40%. These spectroscopy measurements were done in two steps:

a) Single specimen testing – each specimen (SR or ER) was tested singly at 0.1 mHz up to 1 kHz using the sinusoidal voltage of 140 V_{rms}; and

b) Series joined specimen testing – SR and ER specimens were serially connected and bonded by the pressure of the ring electrodes, and the same voltage was applied as in step (a) above.

The IDA instrument collected the data for steps (a) and (b); then, the data were transferred to a PC for further analysis.

EXPERIMENTAL RESULTS

First, the results of dielectric measurements for the single specimen test are presented, and then the dielectric measurements for series joined silicone rubber, and epoxy resin are presented.

Dielectric Characteristics of Single Polymer Specimen

The dielectric losses SR is shown in Figure 4, in which few SR show dielectric loss peaks close to 1 mHz. This has a short span since it turns close to 1 Hz (for laboratory-manufactured samples) and 1000 Hz (for industrial-made samples). The shapes of the curves in Figure 4 of dielectric loss of the samples manufactured in the laboratory (i.e., S1, S2, S481 and S482) look like a loose **S – shape**. Specimens S1 and S2 dielectric losses peak at 0.5 mHz whilst the rest do not, except for S481 and S482, which show a peak close to 0.1 mHz. Specimens PS and SF did not show noticeable peaks at lower frequencies. Note the peak (dielectric loss of 1) attained by specimens S1 and S2 at 0.5 mHz, respectively. Specimens S481 and S482 attained dielectric loss of 2.6 and 1.7 at 1 mHz, respectively. Specimen SF1 attained a dielectric loss of 0.4, and sample PS attained a dielectric loss of 0.8 at 1 mHz, respectively.

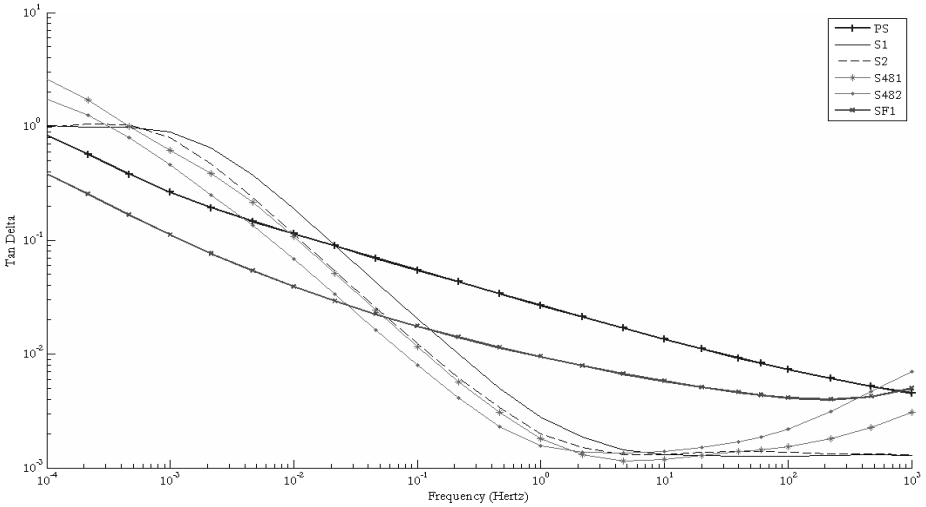

Figure 4: Frequency response of dielectric loss factor of silicone rubber.

All singly tested epoxy resin specimens' dielectric properties are shown in Figure 5. Excluding the lower and higher frequencies, all ER samples exhibit the same characteristics regardless of their curing time and temperatures. Figure 5 notes the values of dielectric loss of specimens E141 and E242 at low frequencies. All specimens have dielectric loss values approximately equal to 0.002 at 1 mHz. Different values are observed at 1000 Hz, with the highest value attained by specimen E482 and the lowest value exhibited by E481. E482 shows the lowest value of dielectric loss at 0.1 mHz, while at the same time, E141 shows the highest value of dielectric loss among the tested polymer samples. Observations of the dielectric curve show at 0.1 mHz specimen with the highest value, i.e., dielectric loss = 0.006925, is E141, and the specimen with the lowest dielectric loss value, i.e.,

dielectric loss = 0.002214 is sample E482. At 1 mHz, dielectric loss values range as loss = 0.001838 (for specimen E481) and dielectric loss = 0.003811 (for specimen E141). At 1000 Hz, the highest dielectric loss is exhibited by E482 i.e., dielectric loss = 0.01378, whilst the lowest value is shown by E481, i.e., dielectric loss = 0.0083553, after which is sample E141, i.e., dielectric loss = 0.0083697.

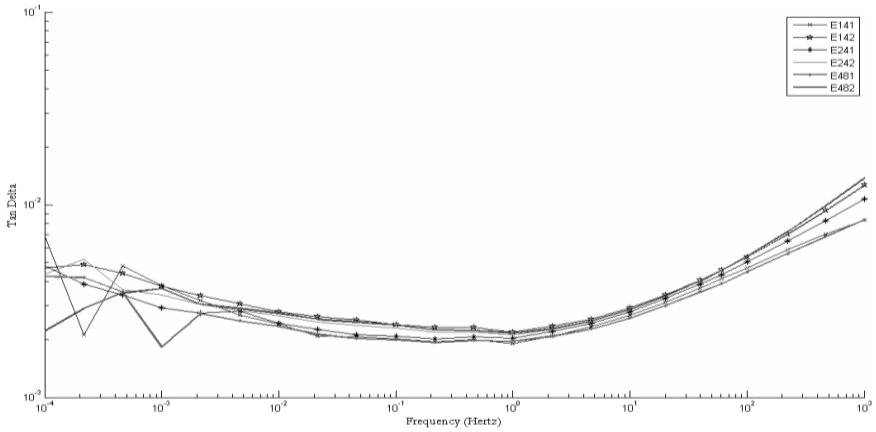

Figure 5: Frequency response of dielectric loss of epoxy resin specimens.

Dielectric Characteristics of Serially Combined Silicone Rubber and Epoxy Resin

When the polymers were combined serially, the dielectric loss curves exhibited are shown in Figure 6. The polymers' names were made by joining the epoxy name to the silicone name, e.g., E141S1 means epoxy specimen E141 is series joined to silicone specimen S1 (Thadei, 2010). Within Figure 6, several facts are observed. First, note the peaks shown by all specimens except specimen E241PS. The highest dielectric loss peak is shown by specimen E241S481 at 1 mHz frequency. The dielectric loss curve of E241PS does not turn at higher frequencies, whilst it increases at lower frequencies. The other specimens' dielectric loss curves peaks congregate between the following frequencies: 0.8 mHz and 1.4 mHz. The specimen that shows the highest dielectric loss value is E241S481 at a frequency of 1 mHz at which the dielectric loss value is 0.11329. Specimen E142S2 is the next, with a dielectric loss peak of 0.009872 at a frequency of 0.046416 Hz. Specimen E482S2 shows a peak at 1 mHz of dielectric loss of 0.25574. At frequencies ranging from 1 Hz to 10 Hz; all curves except that of E241PS show the start of increasing dielectric losses at high frequencies. The dielectric curve of E241PS behaves differently from others as it turns and increases at around 100 Hz. Looking at a frequency of 1 kHz, the curve with the highest dielectric loss value of sample E482S2 is equal to 0.010536, and the one with the lowest value is a dielectric loss equal to that of E142S2 (the value is 0.0052393).

The thicker SR specimens (SF1 and SF2) could not be serially combined with ER for measurements. The reason was the total thickness of the samples would have exceeded the maximum thickness that the resistivity test fixture could hold. A quick look at table 1 shows that the thickness of any SF specimen is 3 mm, and the smallest thickness of the epoxy resin is 1.2 mm. If these two are series joined, then the thickness will be about 4.2 mm. Then, in Figure 7 the losses of series joined specimens being compared to those of its constituents, i.e., SR and ER.

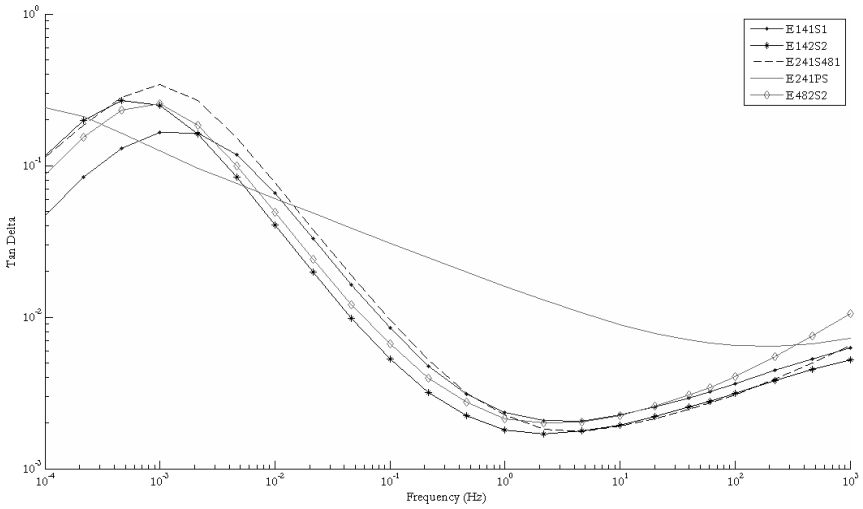

Figure 6: Frequency response of serially connected silicone rubber and epoxy resin.

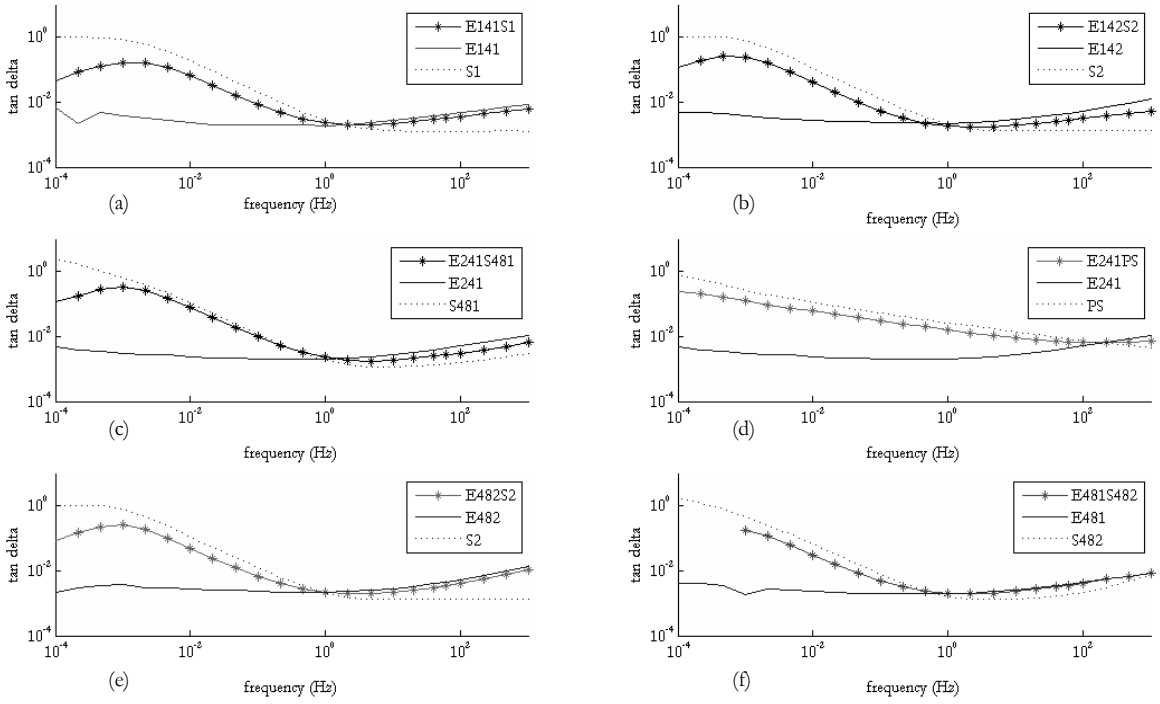

Figure 7: Frequency response of the tested polymer materials.

Note that in Figure 7; for (f), the data displayed by E481S482 was done for a shorter duration than the rest (range of 0.1 mHz and ends at 1 mHz). At 1 Hz is the turning point of all curves except for the case of Figure 7(d). For frequencies higher than 1 Hz, SR has higher dielectric losses than ER and the joined specimens. At frequencies lower than 1 Hz, the ER samples have higher dielectric losses than SR and the joined specimens. Also, looking at all plots, it is seen that the plots of silicone rubber and those of the joined specimens have the same shape signifying that silicone rubber has a stronger influence on the properties of the series of joined specimens. The curves of the joined specimens seem to peak close to where the silicone rubber peak but at a slightly higher frequency than the silicone rubber. The joined specimens have a definite turning point at those lower frequencies. The plot of E241PS shows increasing losses as the

frequency decreases lower than 100 Hz as shown in Figure 7(d).

CONCLUSION

Results of dielectric loss for polymer specimens have been presented for the measurements carried out in room ambient conditions. Silicone rubber specimens industrially manufactured show higher losses than the ones manufactured in the laboratory at frequencies between 10 mHz up close to 1 kHz. This is due to the additives in those specimens manufactured in the industry. It was also found out by reported literature about the effect of filler concentration on the dielectric properties of silicone rubber. The silicone rubbers also show relaxation at lower frequencies which could be due to charge carrier activity. Epoxy resin specimens show similar dielectric losses regardless of their curing time and temperature, showing a minimal tendency towards relaxation at lower frequencies.

The series joined specimens show similar shapes for all specimens, as shown by curves in Figure 6, except for specimen E241PS. The curves of joined specimens are between the epoxy resin specimen and the silicone rubber specimen, as shown in Figure 7. At frequencies lower than 1 Hz, the joined specimen losses are higher than losses for ER and lower than those for SR. At those frequencies starting at 1 Hz, the serially combined samples' dielectric losses are slightly lower than those of ER and higher than those of SR. The dielectric loss curves of the serially combined specimens exhibit a stronger influence of the SR than the ER. In future, the study could investigate accelerated aging of these polymers and the effects of temperature and UV light exposure.

AKNOWLEDGMENT

Support the Sida/SAREC Capacity building project of the University of Dar es Salaam for funding the research up to 2010. Also, Stanislaw Gubanski, Johan Andersson and the Division of High Voltage of Chalmers University of Technology for providing laboratory space and equipment to do the spectroscopy measurements.

REFERENCES

Asokan, A. N., Preetha, P., & Sunitha, K. (2020). Statistical analysis of electric field distribution in insulating nanodielectrics. *IEEE Transactions on Dielectrics and Electrical Insulation*, **27**(2): 549–557. https://doi.org/10.1109/TDEI.2020.008641

Blythe, T., & Bloor, D. (2005). *Electrical Properties of Polymers* (2nd ed.). University Press.

Boudefel, A., & Gonon, P. (2006). Dielectric response of an epoxy resin when exposed to high temperatures. *Journal of Materials Science: Materials in Electronics*, **17**(3): 205–210. https://doi.org/10.1007/s10854-006-6762-2

Bright, C. (2013). Transparent conductive thin films. In *Optical Thin Films and Coatings: From Materials to Applications* (pp. 741–788). Elsevier Ltd. https://doi.org/10.1533/9780857097316.4.741

Capaccioli, S., Butta, E., Corezzi, S., Lucchesi, M., & Rolla, P. A. (1998). *Hopping charge transport in conducting polymers studied by dc conduction and dielectric response analysis* (S. Ducharme & J. W. Stasiak, Eds.; 162–173). https://doi.org/10.1117/12.328156

Choudhary, M., Shafiq, M., Kiitam, I., Hussain, A., Palu, I., & Taklaja, P. (2022). A Review of Aging Models for Electrical Insulation in Power Cables. *Energies*, **15**(9): 3408. https://doi.org/10.3390/en15093408

Dakin, T. W. (2006). Conduction and polarization mechanisms and trends in dielectric. *IEEE Electrical Insulation Magazine*, **22**(5): 11–28. https://doi.org/10.1109/MEI.2006.1705854

de Andrade Raponi, O., Righetti de Souza, B., Miranda Barbosa, L. C., & Ancelotti Junior, A. C. (2018). Thermal, rheological, and dielectric analyses of the polymerization reaction of a liquid thermoplastic resin for infusion manufacturing of composite materials.

Polymer Testing, **71**: 32–37. https://doi.org/10.1016/j.polymertesting.2018.08.024

Ediriweera, S., Jayarathna, P., Samarasinghe, R., & Lucas, R. (2020). Influence of Thickness of Solid Insulators on Creeping Discharges Propagating over Epoxy and Glass Insulators Immersed in Coconut Oil. *2020 IEEE Electric Power and Energy Conference (EPEC)*, 1–6. https://doi.org/10.1109/EPEC48502.2020.9320088

Ehsani, M., Bakhshandeh, G. R., Morshedian, J., Borsi, H., Gockenbach, E., & Shayegani, A. A. (2007). The dielectric behavior of outdoor high-voltage polymeric insulation due to environmental aging. *European Transactions on Electrical Power*, **17**(1): 47–59. https://doi.org/10.1002/etep.119

Francis, U. U., & Philip, A. N. (2022). Degradation of epoxy reinforced Banana fibers and eggshell particles hybrid composite high-voltage insulators via accelerated UV aging processes. *Chemical Data Collections*, *38*, 100842. https://doi.org/10.1016/j.cdc.2022.100842

GE Energy Services. (2007). *GE Energy Services Programma Products*.

Instruments LLC, K. (2019). *Instruction Manual Model 8009 Resistivity Test Fixture*.

Jia, B., Zhou, J., Chen, Y., Lv, Z., Guo, H., Zhang, Z., Zhu, Z., Yu, H., Wang, Y., & Wu, K. (2022). Local charge transport at different interfaces in epoxy composites. *Nanotechnology*, **33**(34): 345709. https://doi.org/10.1088/1361-6528/ac705f

Jonscher, A. K. (1999). Dielectric relaxation in solids. *Journal of Physics D: Applied Physics*, **32**(14): R57–R70. https://doi.org/10.1088/0022-3727/32/14/201

Kumara, S., Pourrahimi, A. M., Soroudi, A., Xu, X., Hammarström, T., Serdyuk, Y., & Müller, C. (2022). Invariant electrical conductivity upon thermal ageing of a crosslinked copolymer blend for high voltage insulation. *Materials Advances*, **3**(11): 4718–4723. https://doi.org/10.1039/d2ma00153e

Kumara, S., Xu, X., Hammarstrom, T., Pourrahimi, A. M., Muller, C., & Serdyuk, Y. v. (2020). Comparison of Different Methods for Characterization of DC Conductivity of Insulating Polymers. *2020 IEEE 3rd International Conference on Dielectrics (ICD)*, 435–438. https://doi.org/10.1109/ICD46958.2020.9342018

Li, C., Chen, G., Qiu, X., Lou, Q., & Gao, X. (2021). A direct proof for Maxwell–Wagner effect of heterogeneous interface. *AIP Advances*, **11**(6): 065227. https://doi.org/10.1063/5.0040947

Li, C., Shahsavarian, T., Baferani, M. A., & Cao, Y. (2021). Tailoring insulation surface conductivity for surface partial discharge mitigation. *Applied Physics Letters*, **119**(3): https://doi.org/10.1063/5.0050456

Mushi, A. T., & Kyaruzi, A. L. (2022). Dielectric Properties of Series Joined Silicone Rubber and Epoxy Resin Formulations. *7th International Conference on Mechanical and Industrial Engineering (MIE'2022)*, **48**.

Nguyen, D. H., Sylvestre, A., Gonon, P., & Rowe, S. (2004). Dielectric properties analysis of silicone rubber. *Proceedings of the 2004 IEEE International Conference on Solid Dielectrics, 2004. ICSD 2004.*, 103-106 Vol.1. https://doi.org/10.1109/ICSD.2004.1350300

Nixdorf, K., & Busse, G. (2001). The dielectric properties of glass-fibre-reinforced epoxy resin during polymerisation. *Composites Science and Technology*, **61**(6): 889–894. https://doi.org/10.1016/S0266-3538(00)00174-3

Ogbonna, V. E., Popoola, A. P. I., Popoola, O. M., & Adeosun, S. O. (2022). A review on corrosion, mechanical, and electrical properties of glass fiber-reinforced epoxy composites for high-voltage insulator core rod applications: challenges and recommendations. *Polymer Bulletin*, **79**(9): 6857–6884. https://doi.org/10.1007/s00289-021-03846-z

Riande, Evaristo., & Díaz-Calleja, Ricardo. (2004). *Electrical properties of polymers*. Marcel Dekker.

Rodríguez-Serna, J. M., & Albarracín-Sánchez, R. (2021). A Study on the Life Estimation and Cavity Surface Degradation Due to Partial Discharges in Spherical Cavities within Solid Polymeric Dielectrics Using a Simulation Based Approach. *Polymers*,

13(3): 324. https://doi.org/10.3390/polym13030324

Seanor, D. A. (1982). *Electrical properties of polymers*. Academic Press.

Seifert, J. M., Stietzel, U., & Karner, H. C. (1998). The ageing of composite insulating materials-new possibilities to detect and to classify ageing phenomena with dielectric diagnostic tools. *Conference Record of the 1998 IEEE International Symposium on Electrical Insulation (Cat. No.98CH36239)*, 373–377. https://doi.org/10.1109/ELINSL.1998.694812

Serdyuk, Yu. V., Podoltsev, A. D., & Gubanski, S. M. (2002). Dielectric properties of 3D composite structures: Simulations versus experiments. *Annual Report Conference on Electrical Insulation and Dielectric Phenomena*, 142–145. https://doi.org/10.1109/CEIDP.2002.1048756

Thadei, A. (2010). *Non-ceramic insulators in Coastal Tropical climates-The case study of Tanzania field performance of polymeric insulators and dielectric characteristics of silicone rubber and epoxy resin formulations* [Masters]. University of Dar es Salaam.

Thadei, A., & Kyaruzi, A. (2008, November). Surface resistivity of silicone rubber formulations tested in room ambient conditions: The case of silicone rubber with and without filler materials. *International Conference on Research and Development*.

Tuncer, E. (2004). *On micro-structural effects in dielectric mixtures*.

Tuncer, E. (2005). Structure–property relationship in dielectric mixtures: application of the spectral density theory. *Journal of Physics D: Applied Physics*, **38**(2): 223–234. https://doi.org/10.1088/0022-3727/38/2/006

Tuncer, E., & Gubanski, S. M. (1999). Filler concentration effects on losses in silicone based polymeric composites. *1999 Annual Report Conference on Electrical Insulation and Dielectric Phenomena (Cat. No.99CH36319)*, 687–690. https://doi.org/10.1109/CEIDP.1999.807898

Tuncer, E., & Gubanski, S. M. (2000). Electrical properties of filled silicone rubber. *Journal of Physics: Condensed Matter*, **12**(8): 1873–1897. https://doi.org/10.1088/0953-8984/12/8/330

Uflyand, I. E., Irzhak, T. F., & Irzhak, V. I. (2022). Formation of fiber composites with an epoxy matrix: state-of-the-art and future development. *Materials and Manufacturing Processes*, **37**(7): 723–747. https://doi.org/10.1080/10426914.2021.2016820

Wang, D., Zhang, G., Zhang, Y., & Chen, S. (2000). Effect of reaction-induced phase separation on dielectric properties of epoxy resin modified with rubber. *Proceedings of the 6th International Conference on Properties and Applications of Dielectric Materials (Cat. No.00CH36347)*, 926–929. https://doi.org/10.1109/ICPADM.2000.876382

Wu, C., Gao, Y., Liang, X., Gubanski, S. M., Wang, Q., Bao, W., & Li, S. (2019). Manifestation of Interactions of Nano-Silica in Silicone Rubber Investigated by Low-Frequency Dielectric Spectroscopy and Mechanical Tests. *Polymers*, **11**(4): 717. https://doi.org/10.3390/polym11040717

Xu, X., Karlsson, M., Gaska, K., Gubanski, S. M., Hillborg, H., & Gedde, U. W. (2017). Robust measurements of electric conductivity in polyethylene based materials: measurement setup, data processing and impact of sample preparation. *Proceedings of the Nordic Insulation Symposium*. https://doi.org/10.5324/nordis.v0i25.2370

Zong, L., Kempel, L. C., & Hawley, M. C. (2005). Dielectric studies of three epoxy resin systems during microwave cure. *Polymer*, **46**(8): 2638–2645. https://doi.org/10.1016/J.POLYMER.2005.01.083